

Brief Reports

Brief Reports are short papers which report on completed research or are addenda to papers previously published in the Physical Review. A Brief Report may be no longer than 3½ printed pages and must be accompanied by an abstract.

Systematics of chemical and structural disorder on band-edge properties of semiconductor alloys

Srinivasan Krishnamurthy, M. A. Berding, and A. Sher
SRI International, Menlo Park, California 94025

A.-B. Chen

Auburn University, Auburn, Alabama 36849

(Received 24 July 1987; revised manuscript received 21 September 1987)

A comparison between the coherent-potential approximation and second-order perturbation theory (SPT) shows that the SPT can be used to calculate the band-edge properties, e.g., band gaps, effective masses, and the low-field alloy scattering of electrons and holes of semiconductor alloys. The SPT is used in a systematic study of the effects of chemical and structural disorder on band-gap bowing and scattering rates near the band edge. The effects of these two disorders can be constructive or destructive, depending on the relative signs of the disorder parameters. Numerical examples are presented for several III-V and II-VI pseudobinary semiconductor alloys.

The crudest approximation for the electronic structure of alloys in the virtual-crystal approximation (VCA) in which the alloy potential is taken as the concentration-weighted average of the constituent potential. The next approximation is second-order perturbation theory (SPT) in which the disorder potential is treated perturbatively as a correction to the VCA result. Perturbation theory, however, is limited to cases where the scattering potential is weak. A frequently used result of multiple-scattering theory is the coherent-potential approximation (CPA).¹⁻³ However, CPA is useful only for cases where the disorder can be written as a sum of the site contributions with respect to the VCA. Although CPA theory can be extended from a single-site approximation to clusters,^{4,5} the range of correlation that it can handle remains limited because of the computational complexities. Perturbation theory does not suffer this restriction, is computationally less demanding, and leads to expressions whose physical interpretation is often transparent. In the literature^{3,6-8} SPT had been used to study the band-edge properties such as bowing a low-field mobility. This report presents the numerical comparison between CPA and SPT and a systematic study of disorder effect on band-edge properties in semiconductor alloys.

In a perturbation calculation, the self-energy Σ in a $A_xB_{1-x}C$ alloy is expressed in the following general form:

$$\Sigma = x(1-x)(U_B - U_A)g(U_B - U_A), \quad (1)$$

where U_A and U_B are the potentials with respect to the VCA at A and B sites, respectively. The evaluation of the VCA Green's function g can follow the usual band-structure techniques.⁹

NUMERICAL COMPARISON

Consider a cation-substitutional alloy such as $Ga_xIn_{1-x}As$. A minimum of 16 orbitals are required if the spin-orbit interaction is included. A convenient set of local orbitals to use are those that have the Γ_6 , Γ_7 , and Γ_8 symmetry about the cation sites. We include the chemical disorder due to the difference in the term value of cations and structural disorder due to the fluctuation of the first-neighbor interactions resulting from bond-length difference. The spin-averaged scattering potential matrix is block diagonal and a typical 2×2 submatrix has the following form:

$$U_B - U_A = \begin{pmatrix} \delta & \Delta \\ \Delta & 0 \end{pmatrix}. \quad (2)$$

For example, for the Γ_6 representation, $\delta = \epsilon_s^B - \epsilon_s^A$ is the difference between the s -term values, and $\Delta = V_2^B(\Gamma_6) - V_2^A(\Gamma_6)$ is the difference of the first-neighbor interactions between the cation s state and the A_1 state constructed from a symmetrical combination of the four surrounding anion hybrids. Because the off-diagonal matrix elements between nearest neighbors scale approximately as $-1/d^2$ (where d is the bond length),¹⁰ in general, $\Delta < 0$ if $d_A > d_B$, and $\Delta > 0$ if $d_A < d_B$. The disorder at the anion site is assumed to be zero.

The 2×2 self-energy matrix for each representation can be written as

$$\Sigma = \begin{pmatrix} \sigma_1 & \sigma_2 \\ \sigma_3 & \sigma_4 \end{pmatrix}. \quad (3)$$

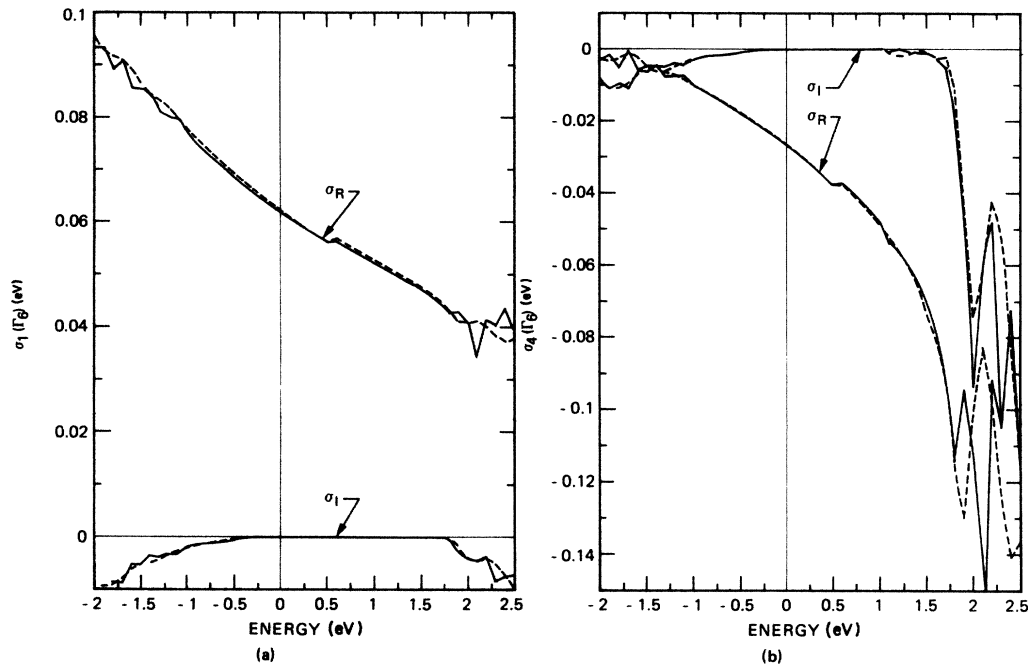


FIG. 1. Comparison between SPT (solid curve) and CPA (dashed curve) for $\text{Ga}_{0.5}\text{In}_{0.5}\text{As}$. (a) Diagonal cation self-energy σ_1 and (b) diagonal anion self-energy σ_4 for the Γ_6 representation.

For cation-substitutional alloys with moderate s -term value differences, the most important part of the self-energy is the σ_1 in the Γ_6 representation, which will affect the s -like conduction-band edge. For anion-substitutional alloys, such as $\text{GaP}_{1-x}\text{As}_x$ and $\text{GaAs}_x\text{Sb}_{1-x}$, in addition to the above self-energies, we have to consider the σ_1 in the Γ_7 and Γ_8 representation affecting the p -like valence-band edge. If the constituent compounds are not nearly lattice matched, σ_2 and σ_3 may also be important. Both CPA and SPT self-energies were calculated for complex energies, and then analytically continued to the real axis.¹¹ For complex energies the Green's functions are relatively smooth functions of energy and the Brillouin-zone integration is facilitated. Computational times for the SPT were about 100 times less than for the CPA.

Figures 1(a) and 1(b) compare CPA and SPT calcula-

tions of the real and imaginary self-energy elements σ_1 and σ_4 of the Γ_6 representation for the cation-substitutional alloy $\text{Ga}_{0.5}\text{In}_{0.5}\text{As}$. Note that this alloy has moderate diagonal and off-diagonal disorder (Table I). We see that SPT and CPA agree well for energies within 2 eV of the band edges. Agreements between SPT and CPA for self-energy components not shown are comparable to those for the components shown. Figures 2(a) and 2(b) show the comparison of SPT and CPA for σ_1 and σ_4 for the Γ_8 representation for the anion-substitutional alloy $\text{InP}_{0.5}\text{As}_{0.5}$. Figure 2 shows that the SPT values are very close to the CPA results even for energies up to 2 eV away from the band edge. These results support the use of SPT for the band-edge properties. The difference between the SPT and CPA becomes larger for energies higher in the conduction bands and also near the bottom of the upper valence bands.

TABLE I. Diagonal, δ , and off-diagonal, Δ , scattering parameters for several III-V and II-VI semiconductor alloys, $A_xB_{1-x}C$. We define $\delta = \epsilon^B - \epsilon^A$ and $\Delta = V_2^B - V_2^A$, where ϵ are the diagonal term values and V_2 are the covalent matrix elements. All energies are in eV.

Alloy	Γ_6 representation		Γ_8 representation	
	δ	Δ	δ	Δ
Cation-substituted alloys				
$\text{Ga}_x\text{In}_{1-x}\text{As}$	0.89	1.05	0.29	0.55
$\text{Ga}_x\text{In}_{1-x}\text{Sb}$	1.25	1.06	0.12	0.26
$\text{Hg}_x\text{Cd}_{1-x}\text{Te}$	1.44	-0.02	0.18	-0.40
$\text{Hg}_x\text{Zn}_{1-x}\text{Te}$	1.00	-0.52	0.25	-0.71
Anion-substituted alloys				
$\text{InP}_{1-x}\text{As}_x$	0.58	-0.26	-0.47	0.35
$\text{GaAs}_x\text{Sb}_{1-x}$	1.50	1.20	0.07	0.56
$\text{InAs}_x\text{Sb}_{1-x}$	1.26	1.08	-0.09	0.31

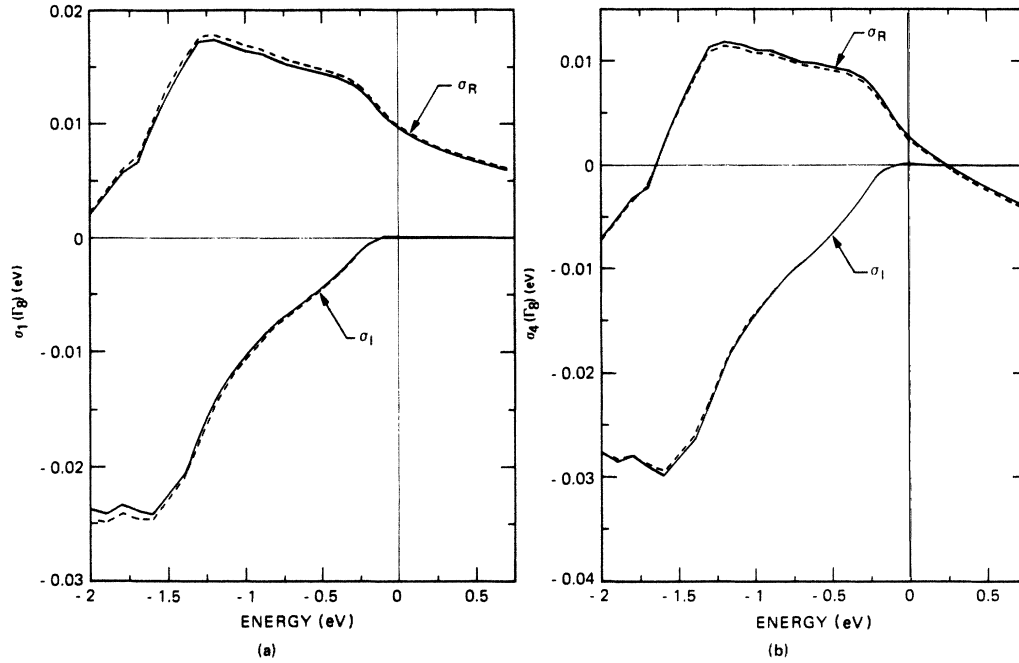


FIG. 2. Comparison between SPT (solid curve) and CPA (dashed curve) for $\text{InAs}_{0.5}\text{P}_{0.5}$. (a) Diagonal cation self-energy σ_1 and (b) diagonal anion self-energy σ_4 for the Γ_8 representation.

BAND-GAP BOWING

When an alloy has both diagonal and off-diagonal disorder, a conclusion might be that these two disorders reinforce each other in their effects on the electronic properties. However, it was pointed out by Hass *et al.*¹² that in the off-diagonal disorder reduces the bowing parameter caused by the diagonal disorder in $\text{Ga}_{1-x}\text{In}_x\text{As}$. We use SPT to show that the interference of these two disorders can be constructive or destructive, depending on the signs of the disorder parameters and on the states considered.

First we consider the shift of the conduction-band edge, δE_c , induced by alloy disorder. To calculate δE_c , we need to know the composition of the state at the bottom of the conduction band calculated in VCA:

$$|\Gamma_6^c\rangle = c|c\rangle + a|a\rangle, \quad (4)$$

where $|c\rangle$ and $|a\rangle$ are the Bloch basis functions at $\mathbf{k}=0$ made of the linear combinations of the Γ_6 cation and anion local orbitals, respectively. δE_c in SPT is given by $\delta E_c = \text{Re}\langle \Gamma_6^c | \Sigma_6 | \Gamma_6^c \rangle$. From Eqs. (1)–(4), we have

$$\begin{aligned} \delta E_c = x(1-x) \{ & |c|^2 \delta^2 + |a|^2 \Delta^2 + 2 \text{Re}(a^*c) \delta \Delta \} f_1 \\ & + [2|c|^2 \delta \Delta + 2 \text{Re}(a^*c) \Delta^2] f_2 \\ & + |c|^2 \Delta^2 f_4 \}, \end{aligned} \quad (5)$$

where f_1 , f_2 , and f_4 are real parts of VCA Green's function, with subscripts denoting matrix element positions as in Eq. (3). We see that the disorder contribution to δE_c is a combination of the disorder parameters δ and Δ , the wave-function expansion coefficients a and c , and f .

For states near the conduction-band edge, f_1 is negative because the conduction band is predominantly cation

s states and the conduction-band states are substantially closer to the conduction-band edge than are the s states, which are at the bottom of the valence bands. Here, f_2 is positive at the conduction-band edge because the numerators tend to be negative for states in the conduction bands (the antibonding states) and positive for the valence-band states (the bonding states). Although the anion Γ_6 partial density of states is greater in the valence bands than in the conduction bands, the conduction-band s states lie closer to the conduction-band edge than to those in the valence bands. The results is substantial cancellation, leading to a small value of f_4 . Table II lists the values of the partial density of states $|c|^2$ and $|a|^2$ and $2 \text{Re}(a^*c)$ for the alloys studied. Note that although the Γ_6^c state is often thought to be derived from the cation s states, our calculation shows that there can be a non-negligible anion contribution.

Now we can proceed to systematically analyze the effects of disorder on the conduction-band bowing. If

TABLE II. Probability densities $|a|^2$ and $|c|^2$ and cross product $2 \text{Re}(a^*c)$ at the bottom of the conduction band of the cation-substituted alloys and at the top of the valence band for the anion-substituted alloys.

Alloy	$ a ^2$	$ c ^2$	$2 \text{Re}(a^*c)$
$\text{Ga}_x\text{In}_{1-x}\text{As}$	0.27	0.73	−0.88
$\text{Ga}_x\text{In}_{1-x}\text{Sb}$	0.44	0.56	−0.99
$\text{Hg}_x\text{Cd}_{1-x}\text{Te}$	0.15	0.85	−0.65
$\text{Hg}_x\text{Zn}_{1-x}\text{Te}$	0.15	0.85	−0.72
$\text{InP}_{1-x}\text{As}_x$	0.99	0.01	0.17
$\text{GaAs}_x\text{Sb}_{1-x}$	0.94	0.06	0.48
$\text{InAs}_x\text{Sb}_{1-x}$	0.96	0.04	0.38

off-diagonal disorder is neglected, i.e., $\Delta=0$, diagonal disorder alone will result in a downward bowing of E_c . This can be seen by examining Eq. (5), where δE_c reduces to $x(1-x)|c|^2\delta^2f_1$, realizing that $f_1 < 0$. When the off-diagonal disorder Δ is not zero and its sign is opposite to that of δ , the effect of Δ will be to increase the downward bowing of E_c ; again this can be seen by examining Eq. (5) and noting that each term will be negative in this case. Finally, if Δ and δ have the same sign, the effect of Δ can be to increase or decrease the bowing, depending on the relative magnitude of Δ and δ .

To calculate the total band-gap bowing, the shift of the valence-band top, δE_v , also has to be considered. δE_v can be expressed in a form similar to that of Eq. (5), except that δ and Δ are the Γ_8 scattering parameters, c and a are reversed and are for the top of the valence band, and f is evaluated at the valence-band edge E_v . Scattering parameters Δ and δ and wave-function coefficients for several III-V and II-VI alloys are given in Tables I and II, respectively. We find that for $\text{Ga}_x\text{In}_{1-x}\text{As}$, $\text{Ga}_x\text{In}_{1-x}\text{Sb}$, $\text{InAs}_x\text{Sb}_{1-x}$, and $\text{GaAs}_x\text{Sb}_{1-x}$, the addition of off-diagonal disorder decreases the total bowing of the band gap. This result from $\text{Ga}_x\text{In}_{1-x}\text{As}$ is consistent with the calculations by Hass *et al.*¹¹ Note that, in $\text{GaAs}_x\text{Sb}_{1-x}$, δ and Δ have different signs in the Γ_8 representation but the same signs in the Γ_6 representation. Therefore, the addition of off-diagonal disorder results in a decrease of the conduction-band bowing while increasing the valence-band bowing by a lesser amount; the result is net decrease in bowing. For $\text{Hg}_x\text{Cd}_{1-x}\text{Te}$, $\text{Hg}_x\text{Zn}_{1-x}\text{Te}$, and $\text{InP}_{1-x}\text{As}_x$, δ and Δ have different signs and diagonal and off-diagonal disorder reinforce each other to increase the total alloy disorder.

ALLOY SCATTERING RATES

The alloy scattering rate R_{alloy} is related to the self-energy through the relationship $R_{\text{alloy}} \propto \text{Im}\langle\psi|\Sigma(E)|\psi\rangle$. Using the relationship $\text{Im}G_{ii}(E) \propto |u_i|^2\rho(E)$, where $\rho(E)$ is the density of states, u is the wave-function expansion coefficient, and G is the full Green's function, we derive an expression for the alloy scattering rate at the conduction-band edge:

$$R_{\text{alloy}}(E_c) \propto x(1-x)\rho(E_c) \times (\delta^2|c|^4 + 4\delta\Delta \text{Re}(a^*c)|c|^2 + 2\Delta^2\{|a|^2|c|^2 + [\text{Re}(a^*c)]^2\}). \quad (6)$$

For $\Delta=0$, the alloy scattering rate is, of course, positive. Since $\text{Re}(a^*c) < 0$ for all the cation-substituted alloys (see Table II), when $\Delta \neq 0$ is included, $R_{\text{alloy}}(E_c)$ will increase if δ and Δ have opposite signs. If δ and Δ have the same sign, $R_{\text{alloy}}(E_c)$ can decrease or increase depending on the relative magnitudes of Δ and δ . Thus, as observed for the band-edge bowing, the presence of off-diagonal disorder can increase or decrease the scattering rate relative to the diagonal-only disorder scattering. Here, as also for the bowing, this reduction is made possible by interference reflected in the cross term $\propto (\delta\Delta)$ in the expression for R_{alloy} .

An expression similar to that of Eq. (6) can be derived for $R_{\text{alloy}}(E_v)$, the alloy scattering rate at the valence-band edge. In this case, the same signs of Δ and δ will result in an increase in $R_{\text{alloy}}(E_v)$, while opposite signs can reduce the scattering rate. For $\text{Hg}_x\text{Cd}_{1-x}\text{Te}$, $\text{Hg}_x\text{Zn}_{1-x}\text{Te}$, and $\text{GaAs}_x\text{Sb}_{1-x}$, the addition of off-diagonal disorder results in an increase in $R_{\text{alloy}}(E_i)$, where i refers to the conduction- (valence-) band edge for the cation- (anion-) substitutional alloys. For $\text{Ga}_x\text{In}_{1-x}\text{As}$, $\text{Ga}_x\text{In}_{1-x}\text{Sb}$, $\text{InP}_{1-x}\text{As}_x$, and $\text{InAs}_x\text{Sb}_{1-x}$, the addition of off-diagonal disorder results in a decrease in $R_{\text{alloy}}(E_i)$.

In conclusion, we have compared the merits of the SPT with CPA and have shown that SPT is suitable for calculating the electronic properties near the band gap. The simple form of SPT is not only convenient in computation but is also useful for a more detailed understanding of the effects of alloy disorder on these properties for several III-V and II-VI alloys. We have demonstrated that off-diagonal disorder can either increase or decrease the bowing of the fundamental gap and the band-edge scattering rates. Off-diagonal disorder is found to increase the band bowing in $\text{Hg}_x\text{Cd}_{1-x}\text{Te}$, $\text{Hg}_x\text{Zn}_{1-x}\text{Te}$, and $\text{InP}_{1-x}\text{As}_x$ and to decrease the bowing in $\text{Ga}_x\text{In}_{1-x}\text{As}$, $\text{Ga}_x\text{In}_{1-x}\text{Sb}$, $\text{InAs}_x\text{Sb}_{1-x}$, and $\text{GaAs}_x\text{Sb}_{1-x}$. Off-diagonal disorder increase alloy scattering rates in $\text{Hg}_x\text{Cd}_{1-x}\text{Te}$, $\text{Hg}_x\text{Zn}_{1-x}\text{Te}$, and $\text{GaAs}_x\text{Sb}_{1-x}$ and decrease them in $\text{Ga}_x\text{In}_{1-x}\text{As}$, $\text{Ga}_x\text{In}_{1-x}\text{Sb}$, $\text{InP}_{1-x}\text{As}_x$, and $\text{InAs}_x\text{Sb}_{1-x}$.

This work was supported in part by U.S. Air Force Office of Scientific Research (AFOSR) Contract No. F49620-85-C-0103 and U.S. National Aeronautics and Space Administration (NASA) Contract NO. NAS1-18232.

¹P. Soven, Phys. Rev. **156**, 809 (1967).

²B. Velický, S. Kirkpatrick, and H. Ehrenreich, Phys. Rev. **175**, 747 (1968).

³H. Ehrenreich and L. M. Schwartz, in *Solid State Physics*, edited by H. Ehrenreich, F. Seitz, and D. Turnbull (Academic, New York, 1976), Vol. 31.

⁴K. F. Freed and M. H. Cohen, Phys. Rev. B **3**, 3400 (1971).

⁵C. W. Myles and J. D. Dow, Phys. Rev. B **25**, 3593 (1982).

⁶P. A. Fedders and C. W. Myles, Phys. Rev. B **29**, 802 (1984).

⁷A. Sher, S. Krishnamurthy, Y.-M.L. Shih, and A.-B. Chen,

Bull. Am. Phys. Soc. **31**, 560 (1986).

⁸R. J. Lambert, K. C. Hess, and H. Ehrenreich, Phys. Rev. B **38**, 1111 (1987).

⁹A.-B. Chen, Phys. Rev. B **16**, 3291 (1977).

¹⁰W. A. Harrison, Phys. Rev. B **24**, 5835 (1981).

¹¹K. C. Hass, B. Velický, and H. Ehrenreich, Phys. Rev. B **29**, 3697 (1984).

¹²K. C. Hass, R. J. Lampert, and H. Ehrenreich, Phys. Rev. Lett. **52**, 77 (1984).